

Adaptive time delay based control of non-collocated oscillatory systems

Michael Ruderman

Abstract—Time delay based control, recently proposed for non-collocated fourth-order systems, has several advantages over an observer-based state-feedback compensation of the low-damped oscillations in output. In this paper, we discuss a practical infeasibility of such observer-based approach and bring forward application of the time delay based controller, which is simple in both the structure and design. Moreover, robust estimation of the output oscillation frequency is used and extended by a bias canceling. The latter is required for positioning the oscillatory passive loads. This way, an adaptive version of time delay-based control is realized that does not require prior knowledge of the mass and stiffness parameters. The results are demonstrated on the oscillatory experimental setup with constraints in the operation range and control value.

I. INTRODUCTION

Multi-mass systems with an oscillatory passive load are common in various control applications. A broad class of such systems can be well approximated by fourth-order dynamics where the first active body includes the whole actuator plant, while the second passive body represents the whole oscillating payload to be controlled. Elastic links, especially those with low damping, make such systems challenging for control. Moreover, if only the load output state is available from the sensor measurements, such systems become non-collocated – that is the objective of our present study. For instance in cranes (see e.g. [1]) and winch systems, the vertical vibration dynamics can become significant due to the elasticities in ropes and cables. Longitudinal oscillations in hoisting systems (see e.g. [2]) are also known to be complex, so that the output oscillation frequency becomes uncertain and valid only close to an operation point. Likewise, the drill-string systems represent an exemplary case of oscillating passive loads (with angular motion), see e.g. [3], while such vibration dynamics becomes even more non-trivial.

In this work, we consider a class of fourth-order non-collocated oscillation systems (Section II), for which stabilization only a noisy sensing of the load output displacement is available. We first discuss in detail a practical infeasibility of the classical observer-based state-feedback design with loop reshaping by location of the poles (Section III). We demonstrate that even a low measurement noise, in combination with constraints of the actuator’s force and displacement, makes such a theoretically sound stabilization less usable. Then, it is shown that the recently proposed time delay based control [4], [5] constitutes a suitable robust alternative for such class of the systems (Section IV). Also,

an online adaptation of the oscillation frequency, required for the control parametrization, is provided, thus extending the robust estimator [5]. Experimental evaluation of the proposed control is shown for the adaptive frequency tuning and also additional external disturbances (Section V). Conclusions are in Section VI. Our design of the time delay based stabilization is simple and relies on consideration in frequency domain. Here we recall that analysis of systems with time delay(s) is manageable also with use of the corresponding transfer functions, see [6]. For analysis of time-delay systems by means of the signal-norms see also [7]. For tutorial and basics of time-delay systems we further refer to [8], [9], [10].

II. NON-COLLOCATED FOURTH-ORDER SYSTEM

A. General framework

We consider a general framework of the non-collocated fourth-order systems as depicted schematically in Fig. 1. The system has an active and a passive body with the mass m and M , correspondingly. The relative motion is actuated by the constrained force $f \in [f_{\min}, f_{\max}]$ and has one degree of freedom in the shifted (against each other) coordinates (z, \dot{z}) and (y, \dot{y}) . Both inertial bodies are connected by an

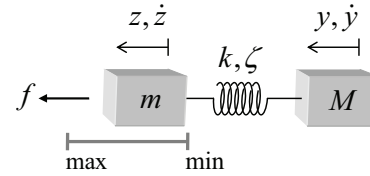


Fig. 1. General framework of non-collocated system.

elastic link (i.e. spring) with the linear stiffness and damping coefficients k and ζ , respectively. In addition, the first active body can be subject to the linear damping σ (equivalent to the viscous friction of an actuator), while the second passive body can be low-damped or even undamped, – a challenging case that we study (also with experiments) in this work. Both moving bodies can be additionally affected by the known constant (or slowly varying) disturbances φ and Φ , each one individually. Further essential assumption is that the active mass has a constrained motion range

$$z \in (z_{\min}, z_{\max}), \quad (1)$$

the fact which is often occurring due to the mechanical limiters of an actuator. With the above assumptions in mind, the motion dynamics inside of the range (1) is given by

$$m\ddot{z} + (\sigma + \zeta)\dot{z} + k(z - y) - \zeta\dot{y} + \varphi = f, \quad (2)$$

$$M\ddot{y} - \zeta(\dot{z} - \dot{y}) - k(z - y) + \Phi = 0. \quad (3)$$

The link damping $\zeta > 0$ is assumed to be relatively low, so that the load motion of an uncontrolled system experiences a long-term oscillatory and undesired for applications behavior in the (y, \dot{y}) coordinates, cf. Fig. 3 below. One of the most challenging characteristics of the system class (2), (3) is the non-collocation of the control value f and the single available output of interest y . Note that the measured $y(t)$ state can additionally be corrupted by the sensor noise. Furthermore, we note that all trajectories in the four-dimensional state-space of (2), (3) are continuous and smooth within (1), while for $z = z_{\min} \vee z_{\max}$ the hard switchings appear, see e.g. [11] for fundamentals of the switched dynamics. This is especially relevant for a constrained motion, addressed later in sections II-B, III-B, as a factor which is inherently limiting the control performance and feasibility.

B. Experimental case study

The experimental case study under consideration is a non-collocated 4th-order mechanical system with gravity, which has a contactless output sensing (Fig. 2). The actuated body is the voice-coil-motor with the bounded input and output

$$u \in [0, 10] \text{ V}, \quad \text{and} \quad z \in [0, 0.021] \text{ m},$$

respectively. An additional actuator's time constant yields

$$f(s) = F(s)u(s) = \frac{\kappa}{\tau s + 1} u(s) = \frac{3.2811}{0.0012s + 1} u(s), \quad (4)$$

written in Laplace domain with the complex variable s . The relative displacement of the passive load is measured by an inductive distance sensor, which has $\pm 12 \mu\text{m}$ nominal repeatability and a relatively large level of noise. The latter is due to a contactless measurement and dynamic misalignments of the moving body with respect to the inductive field-cone of the sensor. Here we recall that there is no bearing for the load mass which is, this way, constituting a free-hanging body, see Fig. 2. Further details about the experimental system can be looked in [12], [5]. For the vector

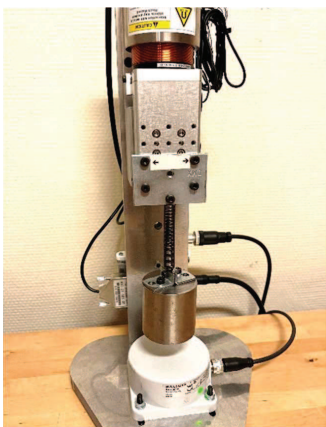


Fig. 2. Experimental setup of the non-collocated system.

of the state variables $x \equiv (x_1, x_2, x_3, x_4)^\top = (\dot{z}, z, \dot{y}, y)^\top$, the state-space model corresponding to (2), (3) is given by

$$\begin{aligned} \dot{x} &= Ax + Bf + D, \\ y &= Cx, \end{aligned} \quad (5)$$

with the matrices and vectors of system parameters

$$\begin{aligned} A &= \begin{pmatrix} -333.35 & -333.33 & 0.015 & 333.33 \\ 1 & 0 & 0 & 0 \\ 0.012 & 266.66 & -0.012 & -266.66 \\ 0 & 0 & 1 & 0 \end{pmatrix}, \\ B &= (1.667, 0, 0, 0)^\top, \quad C = (0, 0, 0, 1), \quad \text{and} \\ D &= (-9.806, 0, -9.806, 0)^\top. \end{aligned}$$

Worth noting is that the disturbance vector D , cf. (2), (3), is composed by the constant gravity terms acting on both moving bodies. Further, we emphasize that the system (5) has one conjugate-complex pole-pair with the natural frequency $\omega_0 = 16.4 \text{ rad/sec}$ and extremely low damping ratio $\delta = 0.031$. The numerical parameter values of the system model are identified, partially from the available technical data-sheets of components and partially through a series of the dedicated experiments, cf. [4], [13]. An exemplary comparison between the measured and modeled output response is shown in Fig. 3 for a free fall scenario. Starting from non-zeros initial conditions and having $u(t) = \text{const}$ for the gravity compensation, the control input is then switched off at $t = 20 \text{ sec}$. This, in a consequence of $u(t) = 0$ for $t > 20$, leads to a fall down of both masses, while $|\dot{z}| < |\dot{y}|$ due to the actuator bearing. Hence, the oscillatory behavior becomes largely excited once $z = z_{\min}$. Note that while the

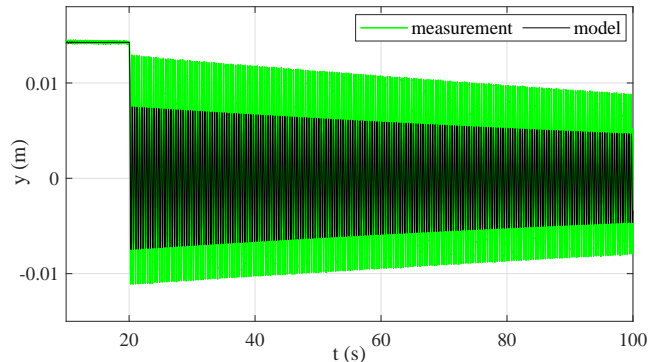


Fig. 3. Comparison of the measured and computed oscillatory response of the free fall scenario ($f(t) = 0$ for $t > 20 \text{ s}$).

oscillation frequency $\omega = \omega_0 \sqrt{1 - \delta^2}$, the damping ratio δ , and the steady-state values of $y(t)$ are well in accord between the measurement and model, the oscillations amplitude is sensitive to both, the initial conditions and exact knowledge of the moving mass and stiffness coefficient, cf. Fig. 3.

III. OBSERVER-BASED STATE-FEEDBACK

A. Theoretical framework

The system dynamics (5), after compensating in feedforward for the known disturbances D , can be arbitrary shaped by the state feedback $-Kx$, provided the control gains $K \in \mathbb{R}^{4 \times 1}$ are designed appropriately. That means the new system matrix $A^* = A - BK$ of the state feedback closed-loop system must be Hurwitz, cf. e.g. [14]. Furthermore, A^* should admit for the real eigenvalues only, in

order to compensate for undesired output oscillations. Note that below, we will consider the state-feedback control part only, i.e. without any pre-filter, correspondingly forward gain applied to the reference value r . This is justified since our main focus (in this section) is on stability and compensation of the oscillations, and not on an accurate reference tracking.

Since $y(t)$ is the only available system measurement, a natural way to keep usage of the state-feedback control is to design an asymptotic state observer [15], also well known as Luenberger (or Luenberger type) observer. The system (5) proves to be fully observable, see e.g. [14], [16], so that an observation gain $Q \in \mathbb{R}^{4 \times 1}$ can be determined so as to provide estimate \tilde{x} of the state vector. The corresponding

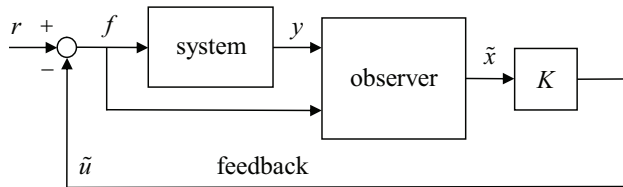


Fig. 4. Block diagram of the state-feedback with observer.

block diagram of a state-feedback control with an observer is then shown in Fig. 4. Recall that for an asymptotically stable observation error $e(t) = x(t) - \tilde{x}(t)$, i.e. for

$$\lim_{t \rightarrow \infty} \|e(t)\| = 0,$$

the system matrix of the observation error dynamics

$$\dot{e}(t) = \tilde{A}e(t) = (A - QC)e(t),$$

must be Hurwitz. For ensuring the asymptotic observer operates efficiently in combination with the state-feedback control, the corresponding poles of \tilde{A} are required (generally) to be significantly faster than those of A^* . Also recall that once the state-feedback, which includes now also the observer, is closed, cf. Fig. 4, the estimate dynamics becomes

$$\dot{\tilde{x}} = (A - BK - QC)\tilde{x} + Bf + Qy. \quad (6)$$

Despite the well-known separation principle when designing the Luenberger observer, that allows the poles of both observer and state-feedback to be assigned independently of each other, a practical realization of the closed-loop as in Fig. 4 reveals less feasible for the system class introduced in section II-A. Next we will show it, although we should emphasize that observer-based state feedback control as in Fig. 4 is well established and accepted in many other types of observable systems (also in applications).

B. Practical feasibility

Even though the designed observer and state-feedback loop based on it have both a stable dynamics of the poles, we are to address additional stability features, that from a loop transfer function point of view, cf. Fig. 4. The observer-based open-loop transfer function from $r(s)$ to $\tilde{u}(s)$ is given by

$$L_o(s) = K(sI - A + BK + QC)^{-1} [BQ] \begin{bmatrix} 1 \\ G(s) \end{bmatrix}, \quad (7)$$

with the identity matrix I of an appropriate dimension and

$$G(s) = C(sI - A)^{-1}B.$$

Note that without use of observer, i.e. if the full state $x(t)$ were measurable, the open-loop transfer function yields as

$$L_m(s) = K(sI - A)^{-1}B. \quad (8)$$

Further we note that in the both above cases, the open-loop transfer functions are not including the additional (disturbing) actuator dynamics $F(s)$, cf. (4). Thus, also the corresponding open-loop transfer functions $F(s)L_o(s)$ and $F(s)L_m(s)$, respectively, must be inspected when analyzing the practical infeasibility. Now, let us make use of the so-called stability margin, or *maximum sensitivity* see e.g. [17] for details, which is defined as the maximum magnitude, i.e.

$$S_{\max} = \max_{\Omega} |S(i\Omega)| = \max_{\Omega} \left| (1 + L(i\Omega))^{-1} \right|, \quad (9)$$

of the corresponding sensitivity function $S(\cdot)$. Recall that the latter is directly related to the open-loop transfer function $L(\cdot)$. Both are evaluated in frequency domain, where Ω in the angular frequency variable and i is the imaginary unit with $i^2 = -1$. Also recall that S_{\max} indicates how close the Nyquist plot of the open-loop transfer function bypasses from the right the critical point $(-1, 0)$ in the complex plane, cf. e.g. [17]. Thus, it represents, to say, a stability capacity of the closed-loop system and is typically required to be $S_{\max} < 2 \approx 6$ dB, cf. [18]. Systems that have the loop transfer function with $S_{\max} > 4 \approx 12$ dB indicate a poor performance as well as poor robustness, cf. [18]. Further we note that for a closed-loop with the structure as in Fig. 4, the sensitivity function represents the transfer characteristics between the reference value and the input to the system plant.

Now consider the design of the above observer and the surrounding state feedback control loop for the system (5) by pole placement. The exemplary assigned poles of the state feedback control are $\lambda_c = \{-40, -42, -44, -60\}$ and those of the asymptotic state observer are $\lambda_o = \{-498, -503, -508, -513\}$. Note that all poles are real and placed sufficiently close to each other, for the observer and controller respectively, thus providing an approximately same time-scale of the natural behavior of the all corresponding states and their estimates. Here, the observer poles are approximately two and a half times faster than those of the closed-loop. All four sensitivity functions, i.e. with and without the use of observer and also with and without the actuator dynamics, are shown in Fig. 5. One can recognize that already the state-feedback without observer has a poor stability margin. When using observer, the S_{\max} peak is further growing and becomes sharper. In case of the actuator dynamics it reaches even 13.4 dB. Recall that a step reference will excite all frequencies, so that the input constraints (cf. section II-A) can then be violated during the transients.

The implemented model (1)–(5) is used in a numerical simulation of the state-feedback control with and without observer designed as above. The simulated output $y(t)$ is subject to a minor (lower than in the experimental system)

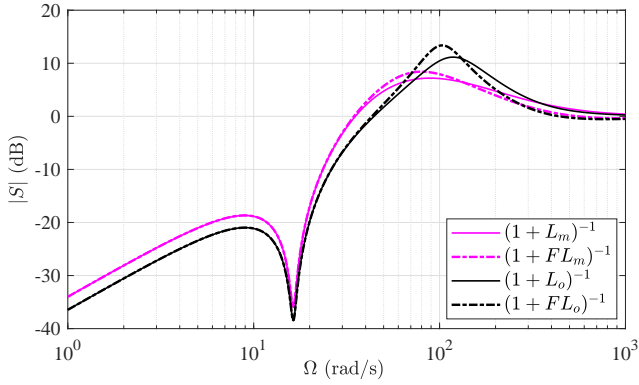


Fig. 5. Sensitivity function of the state-feedback control loop with and without the use of observer.

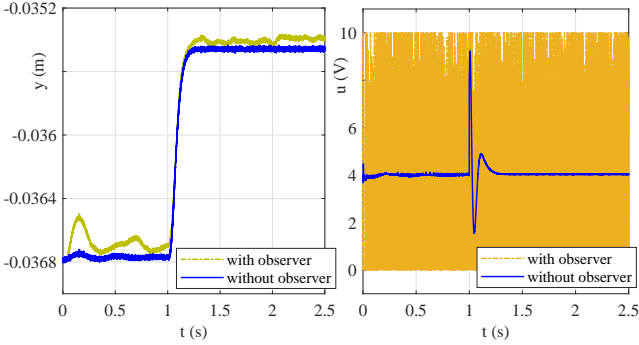


Fig. 6. Simulated response with and without the use of observer.

measurement noise. Also the step reference $r(t)$ is chosen so that the state-feedback control without observer is not saturated, cf. section II-B. The fixed-step solver with the sampling time 0.0002 sec (same as in the real-time experiments) is used. The output response and the control value of the simulation are shown for both cases in Fig. 6. One can see that in case of observer, the control value comes permanently in a high-frequency saturated behavior, that makes the observer-based control practically infeasible.

IV. TIME DELAY BASED CONTROL

A. Time delay based control

The time delay based feedback control of the fourth-order oscillatory systems, initially proposed in [4], was introduced and analyzed in detail in [5], also providing an experimental evaluation in combination with a standard PI (proportional-integral) control. The time delay based control

$$u_d(t) = \alpha(y(t) - y(t - \theta)), \quad (10)$$

relies on the knowledge of the oscillation frequency ω , and assumes the time delay constant

$$\theta = -\arg[G(i\omega)]\omega^{-1}, \quad (11)$$

and the gaining factor $\alpha > 0$. The latter is the design parameter. The system transfer function is given by

$$G(i\Omega) = \frac{y(i\Omega)}{u(i\Omega)} = C(i\Omega I - A)^{-1}B. \quad (12)$$

We note that the time delay based control (10) is largely attenuating the system resonance peak around ω_0 , without much reshaping the $G(i\Omega)$ transfer characteristics at other frequencies. Expressing the transfer function (12) as a ratio $G(i\Omega) = N(i\Omega)P(i\Omega)^{-1}$ of the corresponding polynomials $N(\cdot)$ and $P(\cdot)$, and rewriting (10) in frequency domain as

$$U_d(i\Omega) = \alpha(1 - \exp(-i\Omega\theta)), \quad (13)$$

one can show that the closed-loop $G_{cl} = N(P - NU_d)^{-1}$ is reshaping the system plant transfer characteristics as

$$R(i\Omega) = \frac{G(i\Omega)}{G_{cl}(i\Omega)} = 1 - \frac{N(i\Omega)U_d(i\Omega)}{P(i\Omega)}. \quad (14)$$

The reshaping characteristics (14) of the system frequency response, here without the constant disturbance D and assuming $\tau = 0$ in (4), is exemplary shown in Fig. 7 for $\alpha = 100$. One can recognize that the principal difference

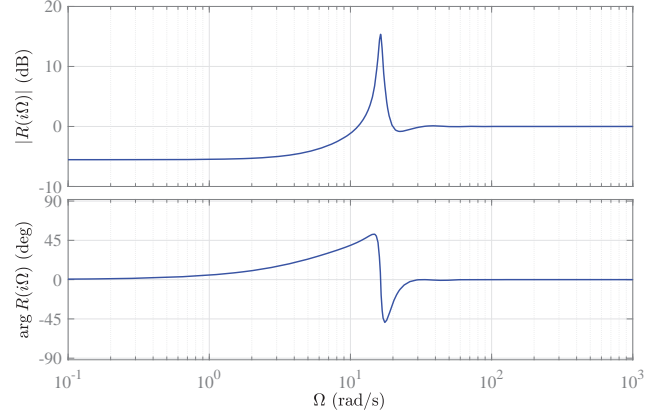


Fig. 7. Reshaping (14) of the system transfer characteristics.

between the original system plant $G(i\Omega)$ and that one with the time delay based compensator, i.e. $G_{cl}(i\Omega)$, is precisely the resonance peak of $G(i\Omega)$. At higher frequencies, there is no changes in the amplitude response, while at lower frequencies an acceptable gain reduction is about -5 dB. This can then be taken into account when the compensated system $G_{cl}(i\Omega)$ will be closed by an outer tracking control, cf. [5]. One can also recognize that the phase response of $G(i\Omega)$ and $G_{cl}(i\Omega)$ are essentially the same to the left- and right-hand-side of the resonance frequency.

B. Robust frequency estimator

The robust frequency estimator, proposed in [12], can be used for an online tuning of the ω -parameter, provided the measured oscillatory signal $w(t)$ in unbiased. The estimator dynamics is given by, cf. [12],

$$\begin{aligned} \begin{pmatrix} \dot{\eta}_1 \\ \dot{\eta}_2 \end{pmatrix} &= \begin{pmatrix} 0 & 1 \\ -\tilde{\omega}^2 & -2\tilde{\omega} \end{pmatrix} \begin{pmatrix} \eta_1 \\ \eta_2 \end{pmatrix} + \begin{pmatrix} 0 \\ 2\tilde{\omega} \end{pmatrix} w, \\ \nu &= (0 \ 1) \begin{pmatrix} \eta_1 \\ \eta_2 \end{pmatrix}, \end{aligned} \quad (15)$$

with the frequency-estimate adaptation law given by

$$\dot{\tilde{\omega}} = -\gamma \tilde{\omega} \text{sign}(\eta_1)(w - \nu). \quad (16)$$

Here $\gamma > 0$ is the gain parameter of the estimation. Note that the right-hand-side of (16) includes (additionally in comparison to [12]) a multiplication with $\tilde{\omega}$, so as to avoid the frequency estimate $\tilde{\omega}$ bypassing into the negative range. For details on the stability and performance of the robust frequency estimator the reader is referred to [12].

In order for a biased oscillation output $y(t)$ can equally be used in the frequency estimator (15), (16), the following dynamic bias-canceling is proposed

$$w(t) = y(t) - y\left(t - \frac{\pi}{\beta}\right), \quad \omega < \beta < 3\omega, \quad (17)$$

where β is a free adjustable time-delay parameter. Assuming a biased, by the term Y_0 , harmonic oscillation

$$y(t) = Y_0 + Y \sin(\omega t + \phi), \quad (18)$$

and substituting it into (17) results in

$$w(t) = Y \left(\sin(\omega t + \phi) - \sin\left(\omega t + \phi - \omega \frac{\pi}{\beta}\right) \right). \quad (19)$$

One can recognize that (19) constitutes also a harmonic signal with the same fundamental frequency ω . The signal is unbiased and has another amplitude and phase comparing to the harmonic part of (18). Also worth noting is that $w(t)$ is not zero signal as long as $\omega\pi\beta^{-1} \neq 0$. If some nominal or upper-bound value of ω is known, the phase shifting factor β can be assigned in a relatively large range, cf. (17). Since the

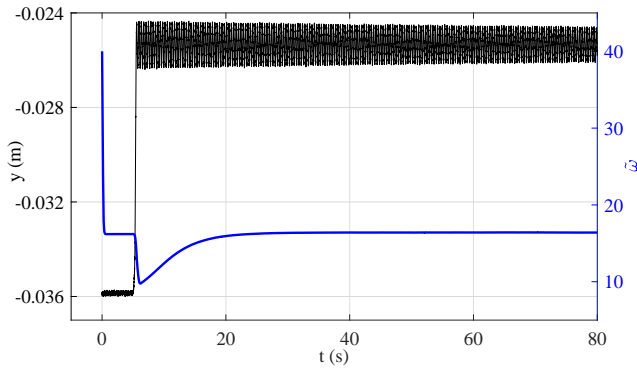


Fig. 8. Converging $\tilde{\omega}(t)$ versus the measured oscillating $y(t)$.

robust estimator (15), (16) is insensitive to both, the phase ϕ and slow variations of Y , see [12], the bias-freed input (19) can directly be used for estimation of $\tilde{\omega}$. Recall that $\tilde{\omega}(t)$ has a convergence behavior which rate is controllable by γ . An exemplary convergence of $\tilde{\omega}$ is shown in Fig. 8, together with the used $y(t)$ measurement. Note that the measured output is biased before and after the step-wise excitation. The initial value is set to $\tilde{\omega}(0) = 40$ and the gain to $\gamma = 200$. One can recognize that after the exciting transient of $y(t)$, the $\tilde{\omega}(t)$ is re-converging towards its final value ≈ 16.4 rad/sec.

V. EXPERIMENTAL CONTROL EVALUATION

A standard PI feedback controller

$$u_{pi}(t) = K_p e(t) + K_i \int e(t) dt, \quad (20)$$

operating on the output error $e(t) = r(t) - y(t)$, with $r(t)$ to be the set reference value for the oscillatory load, can be desirable for the following reasons. (i) The single available system state is $y(t)$. (ii) An integral control action is required for guaranteeing a steady-state accuracy. (iii) An additional differential control action (i.e. resulting in PID control) is not contributing to stabilization of the oscillatory load in the fourth-order system (5). (iv) A state-feedback control, that requires an additional state observer, fails practically for the systems (2), (3), as discussed in detail in section III. At the same time, one can show that the open-loop transfer function $L(i\Omega) = y(s)/r(s) = PI(i\Omega)G(i\Omega)$, where $PI(i\Omega)$ is the transfer function corresponding to (20), has a marginal or even none gain margin. For the basics on gain margin and loop transfer function analysis we refer to e.g. [16]. Also the so-called maximum sensitivity, cf. e.g. [17], will have a relatively high number for the corresponding $S(i\Omega) = (1 + L(i\Omega))^{-1}$, cf. with the analysis made in section III. This indicates a low stability of the closed-loop system.

The overall control law evaluated experimentally is

$$u(t) = u_{pi}(t) + u_d(t) + 4.035, \quad (21)$$

where the last constant term of the right-hand-side compensates for the known gravity disturbance, cf. (2), (3), (4). Note that for the assigned $K_p = 100$, $K_i = 170$, cf. [5], the loop transfer function $L(\cdot)$ without (13) has a sufficient phase margin of 46 deg, but the missing gain margin of -4.2 dB.

First, the closed-loop response controlled with (21) is experimentally evaluated as shown in Fig. 9, once without the time delay control part (i.e. with $\alpha = 0$) and once with the time delay control part with $\alpha = 100$. Note that here a fixed time delay constant, cf. section IV-A, is assigned from the known system parameter ω . While the time delay based

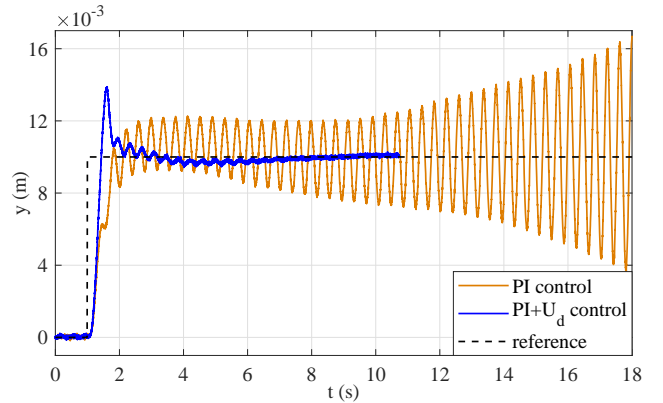


Fig. 9. Measured $y(t)$ controlled by PI (i.e. $\alpha = 0$) and $PI + U_d$ controllers, with $\alpha = 100$ and the fixed θ value.

control provides a relatively fast cancelation of the otherwise oscillating output, cf. also with Fig. 3, the pure PI control drives the system to a visible instability over the time.

Next, the feedback control (21) is experimentally evaluated when applying an online adaptation of θ by means of the robust frequency estimator described in section IV-B. The adaptation gain is assigned to $\gamma = 600$. The results are shown

in Fig. 10, where the controlled output is depicted in (a), and the time progress of the $\tilde{\omega}(t)$ estimate is depicted in (b). Also the manual mechanical disturbances, which are additionally exciting the output oscillations, were applied, once by pushing down and once by pushing up the passive load, see in Fig. 10 (a) marked by the arrows. One can recognize

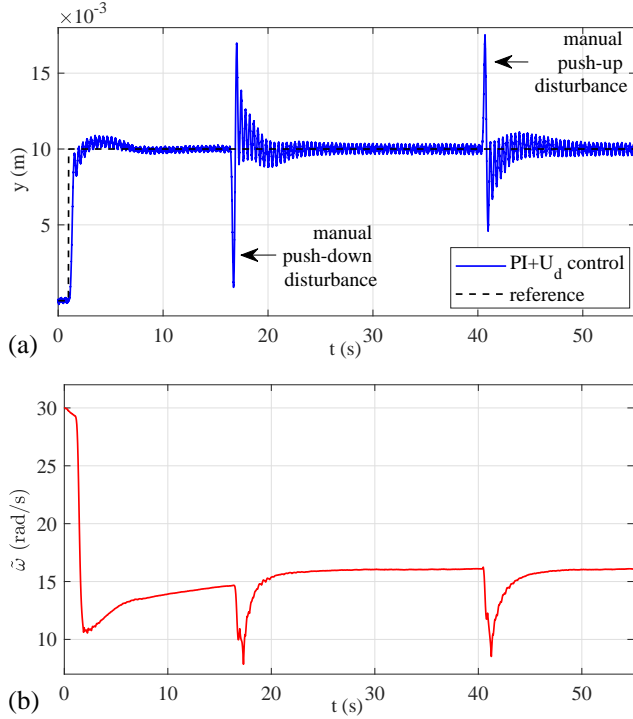


Fig. 10. Measured $y(t)$ controlled with $PI + U_d$ for $\alpha = 100$ and online adapted θ in (a), disturbances are marked; the convergence of $\tilde{\omega}(t)$ in (b).

both, a stable attenuation of the output oscillations and a robust convergence of the $\tilde{\omega}(t)$ estimate. Important to notice is also that due to some (not modeled) nonlinear by-effects in the stiffness, the oscillation frequency ω experiences certain fluctuations depending on the amplitude of $y(t)$, that means on the elongation of the connecting spring.

For further evaluating robustness of the adaptive control (21), i.e. including online estimation of $\tilde{\omega}$, the experiments are performed for oscillatory initial conditions, see Fig. 11. The control parameters are the same as above. One can recognize a largely oscillating $y(t)$ before the step reference is applied. For largely (i.e. more pronounced) oscillations of $y(t)$, the $\tilde{\omega}(t)$ estimate converges faster, which is then perturbed by the output transient with $Y_0 \neq \text{const}$, cf. (18). After transient, the convergence of $\tilde{\omega}(t)$ recovers.

VI. CONCLUSIONS

In this paper, we have addressed the fourth-order non-collocated systems with low-damped oscillating passive loads. Approaching the real applications, an actuator body is subject to the input and output constraints. We analyzed and demonstrated numerically that an observer-based state-feedback control reveals practically infeasible, despite the system dynamics proves to be observable. As a robust

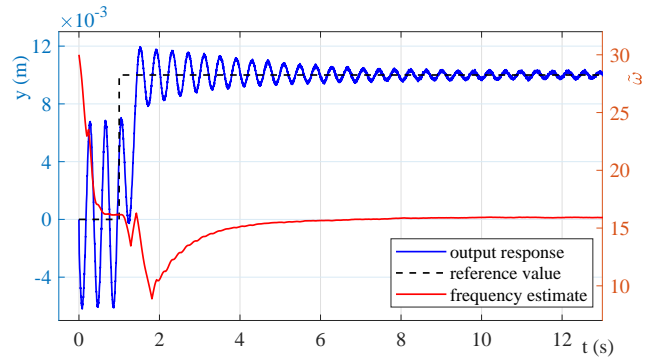


Fig. 11. Measured $y(t)$ controlled with $PI + U_d$ for $\alpha = 100$ and the oscillatory initial conditions, and the convergence of the $\tilde{\omega}(t)$ estimate.

alternative, the time delay based control [4], [5] was applied for stabilizing the otherwise unstable PI controller of the set reference. The bias-canceling extension of the robust frequency estimator [12] was introduced, which allows for an online (adaptive) tuning of the time delay based controller. Various dedicated experiments were shown as confirmatory.

REFERENCES

- [1] J. Vaughan, D. Kim, and W. Singhose, "Control of tower cranes with double-pendulum payload dynamics," *IEEE Transactions on Control Systems Technology*, vol. 18, no. 6, pp. 1345–1358, 2010.
- [2] J. Wang and W. T. van Horssen, "On resonances and transverse and longitudinal oscillations in a hoisting system due to boundary excitations," *Nonlinear Dynamics*, vol. 111, pp. 5079–5106, 2023.
- [3] B. Besselink, T. Vromen, N. Kremers, and N. Van De Wouw, "Analysis and control of stick-slip oscillations in drilling systems," *IEEE Trans. on Control Systems Technology*, vol. 24, no. 5, pp. 1582–1593, 2015.
- [4] M. Ruderman, "Robust output feedback control of non-collocated low-damped oscillating load," in *IEEE 29th Mediterranean Conference on Control and Automation (MED)*, 2021, pp. 639–644.
- [5] M. Ruderman, "Time-delay based output feedback control of fourth-order oscillatory systems," *Mechatronics*, vol. 94, p. 103015, 2023.
- [6] C.-Y. Kao and B. Lincoln, "Simple stability criteria for systems with time-varying delays," *Automatica*, vol. 40, no. 8, pp. 1429–1434, 2004.
- [7] E. Fridman and U. Shaked, "Input–output approach to stability and l2-gain analysis of systems with time-varying delays," *Systems & Control Letters*, vol. 55, no. 12, pp. 1041–1053, 2006.
- [8] K. Gu, V. Kharitonov, and J. Chen, *Stability of time-delay systems*. Springer, 2003.
- [9] W. Michiels and S.-I. Niculescu, *Stability, control, and computation for time-delay systems: an eigenvalue-based approach*. SIAM, 2014.
- [10] E. Fridman, "Tutorial on lyapunov-based methods for time-delay systems," *Eur. Journal of Control*, vol. 20, no. 6, pp. 271–283, 2014.
- [11] D. Liberzon, *Switching in systems and control*. Springer, 2003.
- [12] M. Ruderman, "One-parameter robust global frequency estimator for slowly varying amplitude and noisy oscillations," *Mechanical Systems and Signal Processing*, vol. 170, p. 108756, 2022.
- [13] B. Voß, M. Ruderman, C. Weise, and J. Reger, "Comparison of fractional-order and integer-order H-infinity control of a non-collocated two-mass oscillator," *IFAC-PapersOnLine*, vol. 55, pp. 145–150, 2022.
- [14] P. Antsaklis and A. Michel, *A Linear Systems Primer*. Birkhäuser Boston, 2007.
- [15] D. Luenberger, "An introduction to observers," *IEEE Transactions on Automatic Control*, vol. 16, no. 6, pp. 596–602, 1971.
- [16] G. Franklin, J. Powell, and A. Emami-Naeini, *Feedback control of dynamic systems*. Pearson, 2020.
- [17] K. J. Åström and R. M. Murray, *Feedback systems: an introduction for scientists and engineers*. Princeton University Press, 2021.
- [18] S. Skogestad and I. Postlethwaite, *Multivariable feedback control: analysis and design*. John Wiley & Sons, 2005.